CHAPTER IV
RESULTS AND DISCUSSION

4.1 Characterization of Titanium Glycolate Precursor

Characterization of the precursor using TGA, figure 4.1, shows thermal stability of titanium glycolate giving a decomposition transition at ~360°C, corresponding to the decomposition of ethylene glycol ligand. The final ceramic yield was 48.08% close to the theoretical ceramic yield of 47.52 % (Phonthammachai *et al.*, 2003). This result suggests that the final Ti precursor was quite pure.

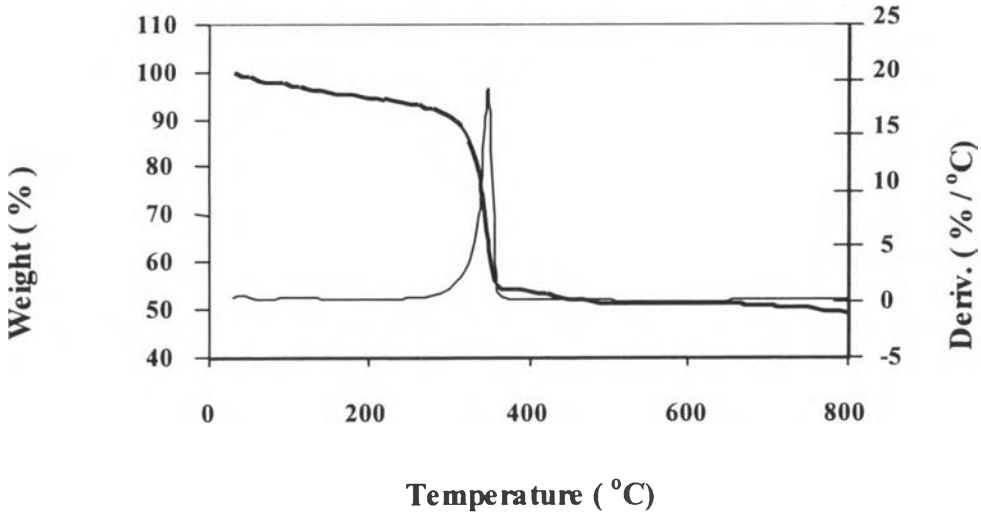

Figure 4.1 TGA/DTG of Ti precursor.

FT-IR spectrum also shows the characteristics of the precursor (Figure 4.2) at 2927-2855 cm^{-1} (νC-H), 1075 cm^{-1} (νC-O-Ti bond) and 619 cm^{-1} (νTi-O bond) (Phonthammachai *et al.*, 2003).

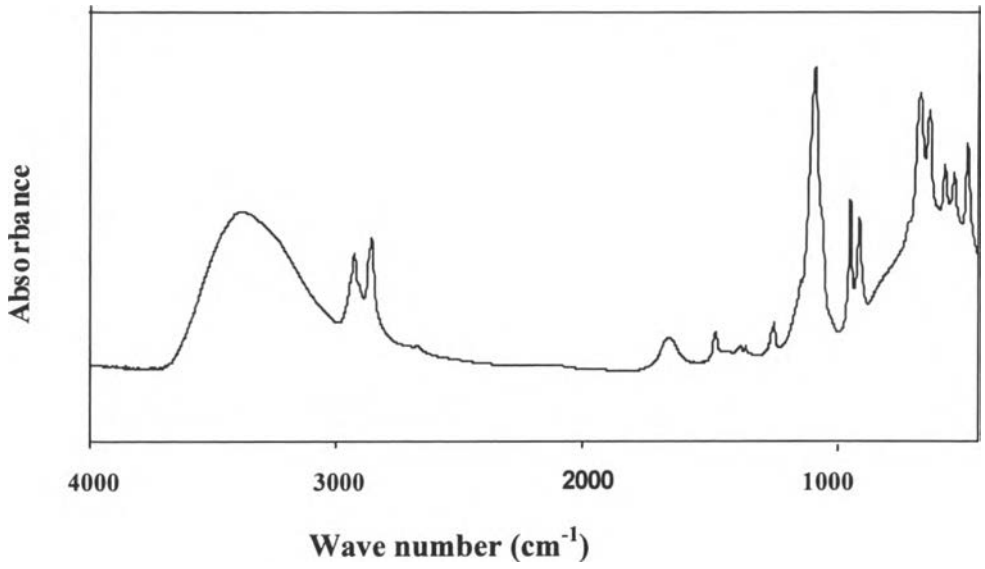

Figure 4.2 Infra-red spectrum of Ti precursor.

4.2 Characterization of Zirconium Glycolate Precursor

Figure 4.3 presents the thermogram of zirconium glycolate, generating 3 decomposition peaks. The first peak at ~70°C refers to the decomposition of acetronitrile residue. The second peak is the major peak giving a mass lost of ethylene glycol ligand at ~420°C. The last endothermic peak around 720°C probably belongs to the decomposition of zirconium carbonate. The final ceramic yield of Zr precursor was 49.59% compared with the theoretical ceramic yield of 52% (Ksapabutr *et al.*, 2004). If the first was filtered off, the obtained ceramic yield of 52.69 % would be very close to the theoretical one.

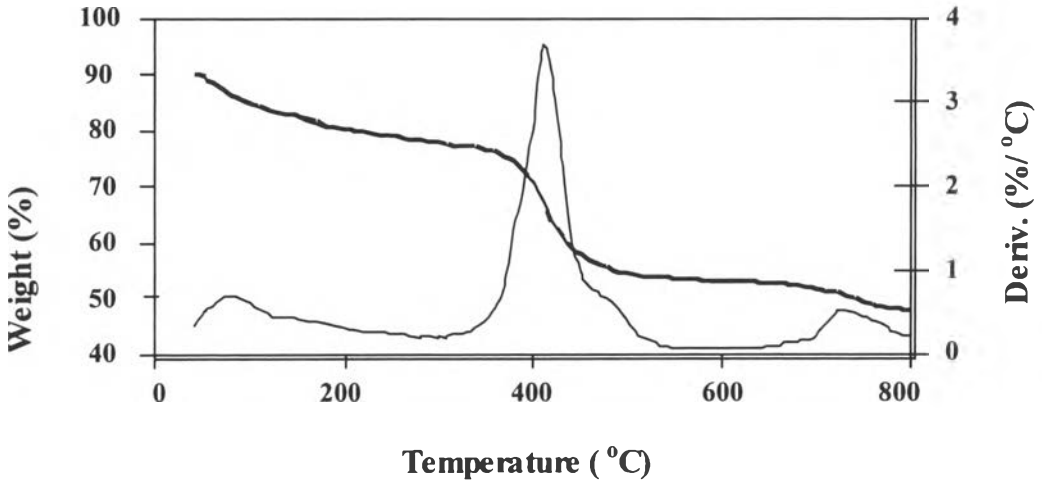

Figure 4.3 TGA/DTG of Zr precursor.

Figure 4.4 shows FT-IR of Zr precursor indicating the functional groups at 2927-2855 cm^{-1} (νC-H), 1090 cm^{-1} (νZr-O-C) and 896, 613 cm^{-1} (νZr-O) (Dage *et al.*, 1997 and Ksapabutr *et al.*, 2004).

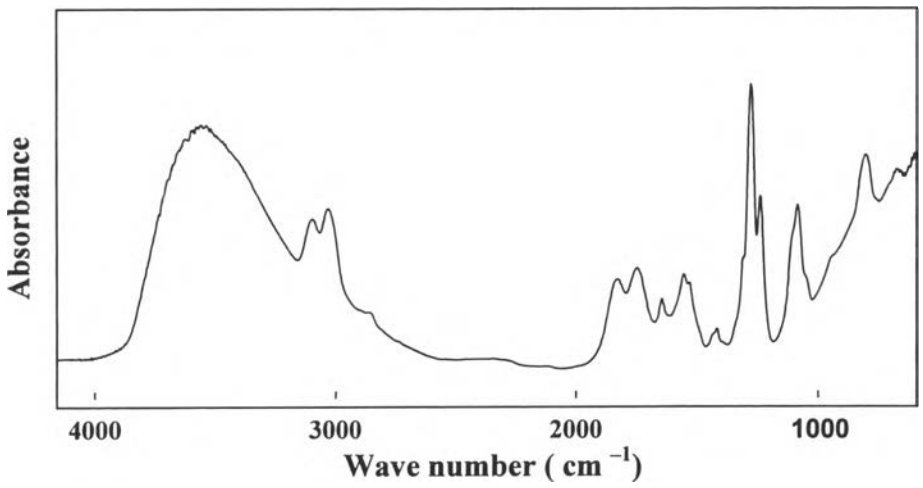

Figure 4.4 Infra-red spectrum of Zr precursor.

4.3 Characterization of Lead Glycolate Precursor

The TGA of the last precursor, lead glycolate, is shown in Figure 4.5. Only one decomposition transition was observed at ~370°C, representing the oxidation decomposition of ethylene glycol ligand. The final ceramic yield was 80 % and can be compared with the theoretical ceramic yield of 89.50%. The main reason for obtaining lower ceramic yield is that the analysis was conducted from ambient to 800°C which is the boiling point of PbO; as a consequence partial ceramic yield was lost during the analysis.

Figure 4.6 shows FT-IR spectrum of the lead glycolate giving functional groups at 2826-2782 (νC-H), 1069 (νPb-O-C) and 683, 574 cm^{-1} (νPb-O) (Dage *et al.*, 1997). The spectrum shows distinguishable characteristics of the lead precursor as compared to the spectrum obtained from lead acetate due to the moisture instability of the lead acetate. Unlike our synthesized lead glycolate, it is moisture stable and thus quite useful for further study.

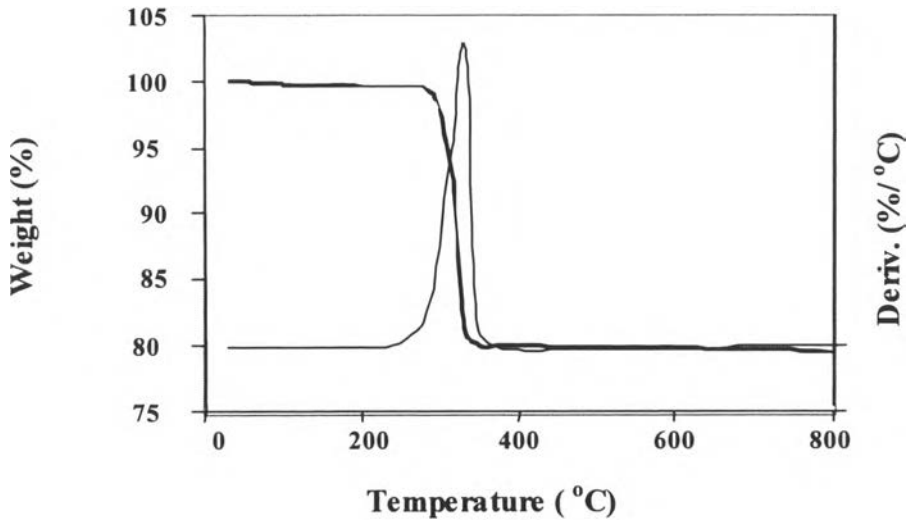

Figure 4.5 TGA/DTG of Pb precursor.

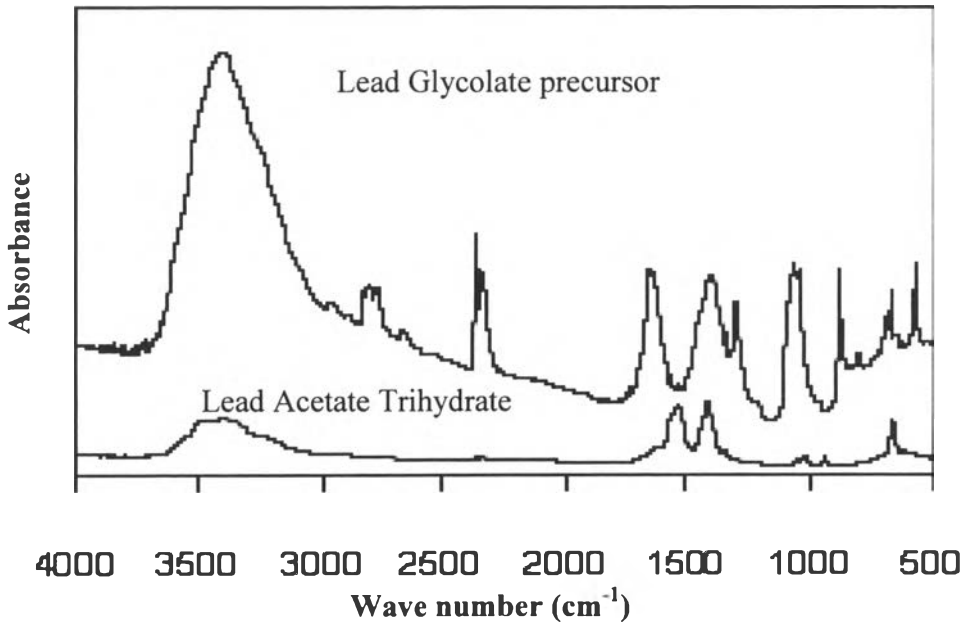

Figure 4.6 Infra-red spectra of lead glycolate and lead acetate trihydrate.

4.4 Optimal Condition for the PZT Gel Formation

First, the proper amount solvent for gel to form was investigated. It was found that acetic acid (Yi and Sayer, 1996) a mixture of acetic acid and sodium hydroxide (Schwartz *et al.*, 1997), nitric acid, and a mixture of nitric acid and sodium hydroxide can dissolve all three precursors to form sol in the first step. Next, we investigate the effects of concentration, pH and temperature on transparent gel formation. If only acetic acid or only nitric acid was employed, the gel will not form either at room temperature or at 50°C. The mixture of 2.5 M HNO_3 + 2.5 M NaOH at pH 3 allowed gels to occur at higher temperature for 1.5 h, as can be seen in Table 4.1 and these are the suitable conditions selected for the next experiment.

Table 4.1 Variation of pH, concentration and temperature for the gel formation

Types of solvent	Concentration (M)	pH	Room temperature	50°C
Acetic acid + Sodium hydroxide	2.5+2.5	2, 3, 4	X, X, X	Condense gel
	5+5	2, 3, 4	X, X, X	Condense gel
Nitric acid + Sodium hydroxide	0.5+0.5	2, 3, 4	X, X, X	X, X, X
	1+1	2, 3, 4	X, X, X	X, X, X
	1.5+1.5	2, 3, 4	X, X, X	Gel at pH3 (10-12 h)
	2+2	2, 3, 4	X, X, X	Gel at pH3 (8.5-10 h)
	2.5+2.5	2, 3, 4	X, X, X	Gel at pH3 (5-7 h)
	3+3	2, 3, 4	X, X, X	Gel at pH3 (1.5-3 h)
	5+5	2, 3, 4	X, X, X	Gel at pH3 (0.5-1.5 h)

where X means no gel formation

From Table 4.1, the best condition for the gel formation is to use the solvent mixture of 2.5M HNO_3 + 2.5M NaOH at 50°C. The next step was to determine a suitable volume ratio of both 2.5M HNO_3 and 2.5M NaOH at different temperature ranging from 40°-90°C. As tablated in Table 4.2, at the temperature of 40°C no gel formed. For acid concentrations higher than 2.7, no gel formed.

Table 4.2 Variation of volume ratio of 2.5M nitric acid/ 2.5M sodium hydroxide and temperature at pH 3 for the gel formation

Volume ratio of HNO_3+NaOH	Temperature (°C)/Time			
	40	50	70	90
1.7	X	Condense gel	Condense gel	Condense gel
1.9	X	Condense gel	Condense gel	Condense gel
2.1	X	Gel/1.5 h	Condense gel	Condense gel
2.3	X	Gel/3 h	Gel/1 h	Condense gel
2.5	X	Gel/5-7 h	Gel/2-3 h	Gel/0.5-1h
2.7	X	X	Gel/4-5 h	Gel/1-2 h
2.9	X	X	X	Gel/3-5 h
3.1	X	X	X	X

Most studies (Dage *et al.*, 1997 and Budd *et al.*, 1985) prepared PZT via the sol-gel process and used precursors that are sensitive to moisture and air. The reaction needed much longer time and higher temperature to complete since those precursors were hydrolyzed and converted to individual metal oxides. For example, Schwart *et al.* (1997) prepared the precursor solution for PZT using titanium isopropoxide, zirconium n-butoxide-butanol and lead (IV) acetate as precursors and methanol, acetic acid and water as solvents. However, the precursors were too moisture sensitive, thus the mixture was

heated to 85°C to dissolve the precursors and allow the reaction to occur. Another example is the work of Hyun Tae Lee et al (Lee *et al.*, 2002). They synthesized PZT by first refluxing lead acetate trihydrate in 2-methoxyethanol, which is a toxic solvent, at 120°C for 4 h. Titanium isopropoxide and zirconium propoxide dissolved in 2-methoxyethanol were then added and the reaction mixture was continued by refluxing at 120°C for another 4 h. By comparing with our PZT synthesis using moisture stable Pb, Ti and Zr glycolates, our reaction condition used is much milder: shorter reaction time (3 h), lower reaction temperature (50-60°C).

4.5 Characterization of PZT Gel Formation as a Function of Time During the Sol-Gel Process

Figure 4.7 shows FTIR spectra of PZT sol in 2.5 M of HNO_3 and 2.5 of NaOH solvent adjusted for pH = 3 and heated at 50°C at various times. At the first stage of 10-30 min PZT sol showed peaks at 3000-2800 cm^{-1} (broad O-H), 2830, 1456 and 1380 cm^{-1} (broad C-H), 1282-1272 cm^{-1} (N-O) [22], 1090-1050 cm^{-1} (broad C-O-M) [3] and 800-400 cm^{-1} (M-O) [23], where M represents Pb, Ti or Zr. 1-2 h PZT gel showed stronger and sharper peaks of C-H at 1456 and 1380 cm^{-1}[23], C-O-M at 1080-1020 cm^{-1} [23]while the M-O peaks at 800-400 cm^{-1} [23] was not observed. 3-4 h PZT gel was harder and provided peaks of C-H, C-O-M and M-O. 5-6 h PZT gel was the hardest gel, and it gave the sharpest, strongest and highest absorbance peak of O-M at 800-400 cm^{-1}[23]. As time increased, PZT gel reversed to be sol, as shown in FTIR spectrum of 8-10 h gel, it has weaker peaks of M-O, as compared to those of the spectrum obtained from the 5-6 h gel. Our results are in agreement with the work of Zhang *et al.* (2003) and Dage *et al.* (1997).

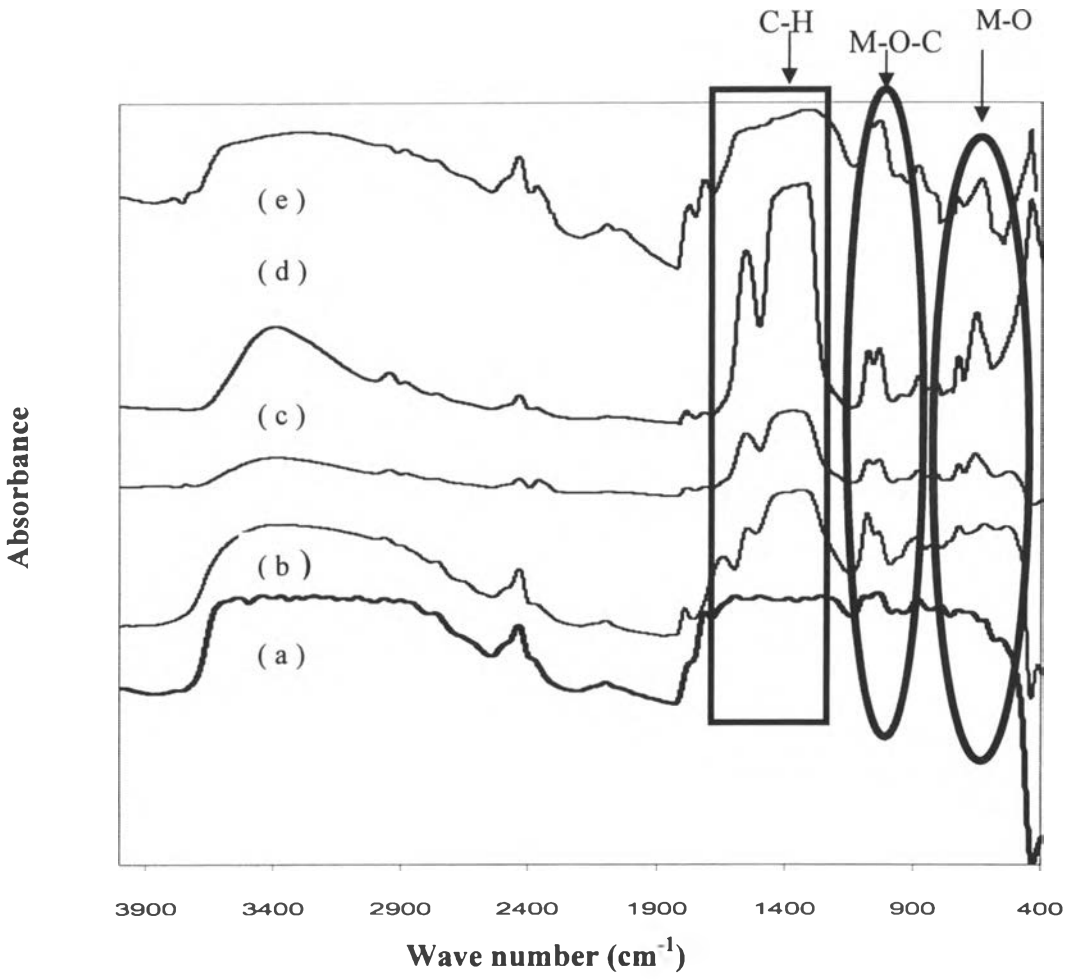

Figure 4.7 FTIR spectra of the PZT gel obtained at (a) 10-30 min, (b) 1-2 h, (c) 3-4 h, (d) 5-6 h and (e) 8-10 h gel time.

4.6 Characterization of Uncalcined PZT Powder Obtained by the Sol-Gel Process

The white powders obtained from all HNO_3 and NaOH ratios and the preheated gels were analyzed using FTIR. The spectra are nearly the same, as shown in Figure 4.8 and Table 4.3, indicating the metal-oxygen-carbon vibration of all metal precursors.

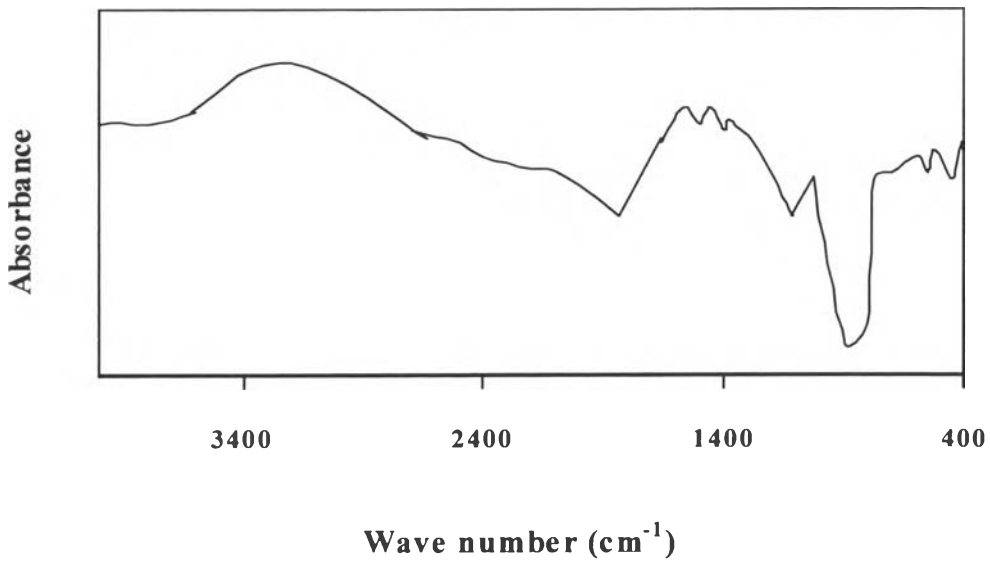

Figure 4.8 FTIR of uncalcined PZT by the sol-gel process.

Table 4.3 M-O-C vibrations of uncalcined PZT

Assignment	Frequency (cm^{-1})
Ti-O-C	1075
Zr-O-C	1090
Pb-O-C	1069

From Figure 4.8, FTIR spectra of uncalcined PZT obtained by the sol-gel process and dried at 110°C for 3 h showed a small C-H peak at 1450-1380 cm^{-1}, indicating that PZT still had residue organic groups. At 110°C complete formation of PZT did not occur. This has been previously shown from the work of R. Caruso et al (Caruso *et al.*, 1999) synthesizing uncalcined PZT or PZT precursor powder by drying PZT precursor solutions in an open flask at 120°C under a normal atmosphere for 24 h and analyzing by FTIR. They also showed some residue organics groups. To obtain complete PZT formation, the preheated PZT had to go through a calcination at high temperature. The suitable temperature was determined by studying the thermal properties of uncalcined PZT or PZT precursor using TGA and DTG, as shown in

Figure 4.9. The first exothermic peak in the temperature range of 200°-400°C was the residual organic groups (Caruso *et al.*, 1999). The last two exothermic peaks were also accompanied by a mass loss and changes in the DTG. The peak at 400°-500°C indicates the pyrochloric phase formation (Livage *et al.*, 1994), while the other at 600°-700°C corresponds to the perovskite phase formation (Dimos *et al.*, 1994). The small exothermic peak above 800°C has been attributed to the PbO volatilization (Saha and Agrawal, 1992 and Chang *et al.*, 2002). This means that the perovskite PZT was formed at high temperature around 700°C.

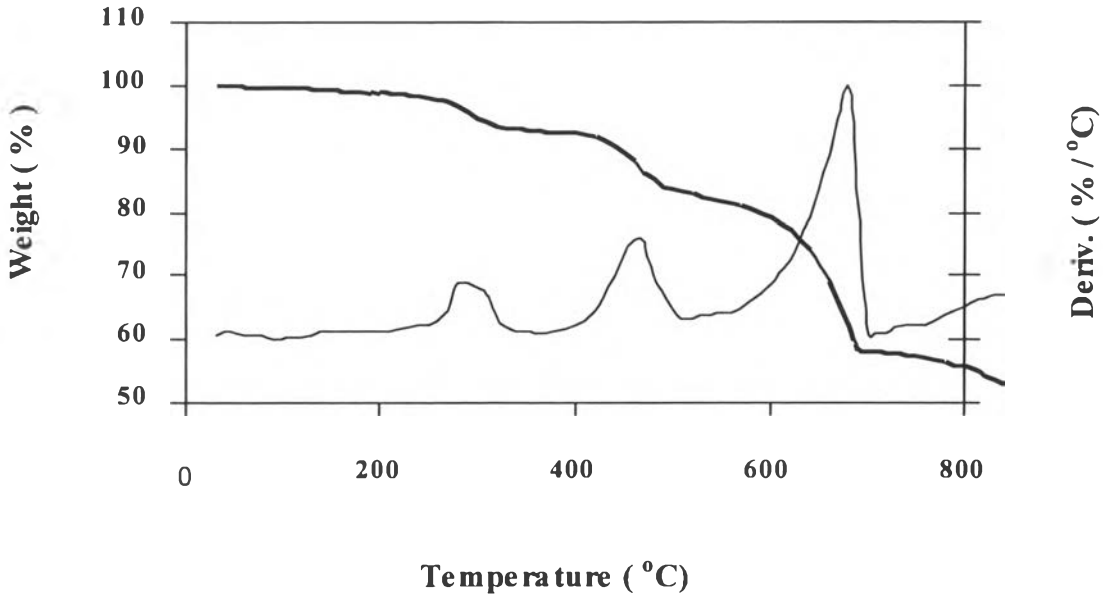

Figure 4.9 TGA/DTG of uncalcined PZT by the sol-gel process.

SEM micrograph of uncalcined PZT is given in Figure 4.10. The morphology of uncalcined PZT clearly appear to be an amorphous phase; at this step the crystalline PZT has not yet formed.

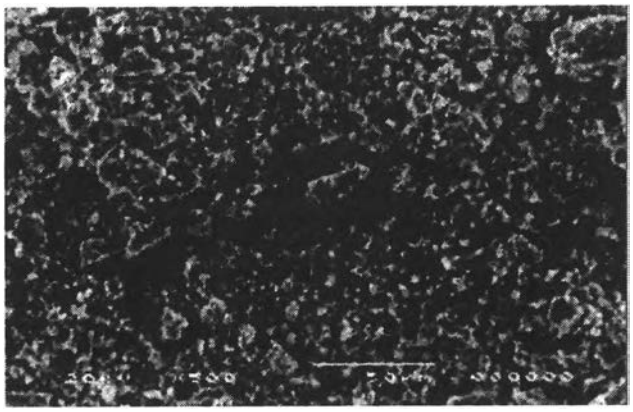

Figure 4.10 SEM of uncalcined PZT by the sol-gel process.

4.7 Characterization of Calcined PZT Powder Obtained by Sol-Gel Process

FTIR spectra of PZT powders calcined at 400°-800°C for 1 h, 1.5 h and 2 h were taken. Figure 4.11 shows a spectrum of a PZT example calcined at 800°C; it has no organic peaks. The assignments of all metal-oxygen vibrations are summarized in Table 4.4.

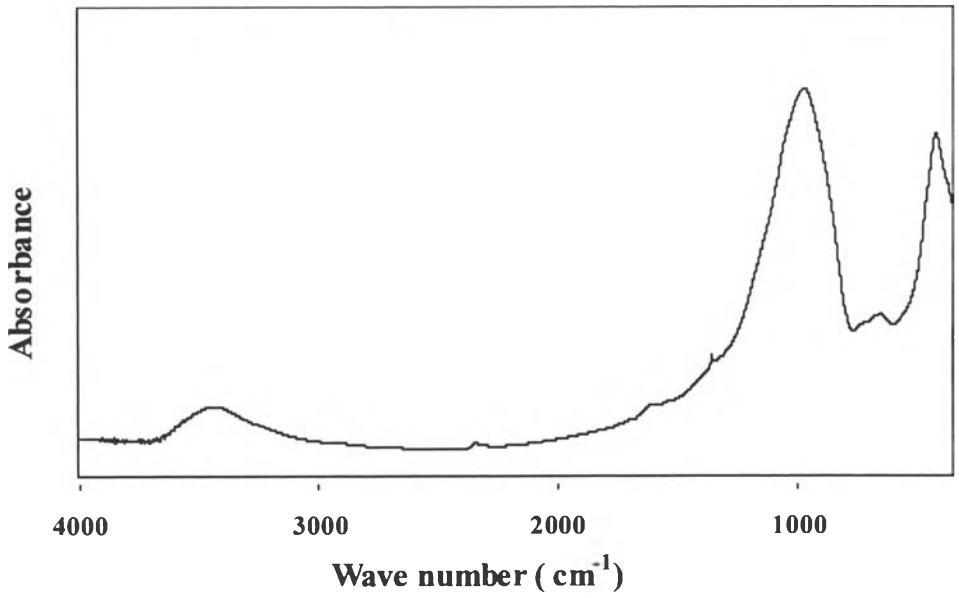

Figure 4.11 FTIR of the PZT powder calcined at 800°C for 1.5 h.

Table 4.4 M-O vibrations of calcined PZT

Assignment	Frequency (cm^{-1})
Ti-O	**691**
Zr-O	**459**
M-O-M	**1004**

where M = Ti or Zr or Pb

Figure 4.12 is the SEM micrograph of macromolecule of calcined PZT at 800°C. The crystal size is much larger than that of uncalcined PZT. Schwartz *et al.* (1997) and Chang *et al.* (2002) studied PZT from SEM and found that with a proper temperature the grain size and the density surface decreased with temperature. However, from our study the grain size and the density surface of PZT increased with temperature.

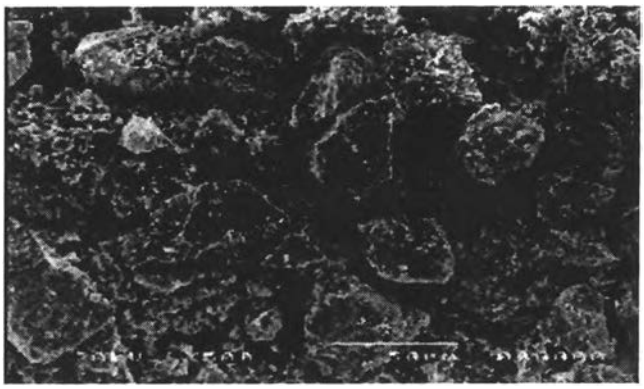

Figure 4.12 SEM morphology of calcined PZT by the sol-gel process.

The density surface of PZT by the sol-gel process was determined by analyzing the surface area value using BET analyzer, see Table 4.5 At higher temperature the surface area decreased, resulting in the increase in the density surface and crystallinity. This indicates that PZT synthesized from Pb, Ti and Zr glycolate precursors is stable at higher temperature.

Table 4.5 Surface area of calcined PZT by the sol-gel process

Temperature of calcined (°C)	Surface area (m^2/g)
700	67.89
800	50.31
900	29.06

XRD patterns of calcined PZT by the sol-gel process are shown in Figure 4.13. In this case, the intensity of X-ray diffraction was used to determine the phase development. The pyrochlore phase was found to be amorphous state at low calcination temperature, as shown in Figure 4.13 (a,b), but at a higher temperature of calcination, the perovskite peaks became sharper and stronger, indicating better crystallinity. The relative intensities of the XRD peaks summarized in Table 4.6 correspond to the Pe (222) and Py (110), which are used to calculate the percentage of perovskite content from equation (1.2) (Lee *et al.*, 2002) when Pe is a perovskite and Py is a pyrochlore.

Table 4.6 Relative intensity of XRD peaks of calcined PZT by the sol-gel process

Calcination Temperature (°C)	Intensity (cps)		Perovskite Content (%)
	Pe (110)	Py (222)	
600	422	312	56.52
700	1154	466	71.24
800	805	-	100.00
900	1075	-	100.00
1100	651	-	100.00

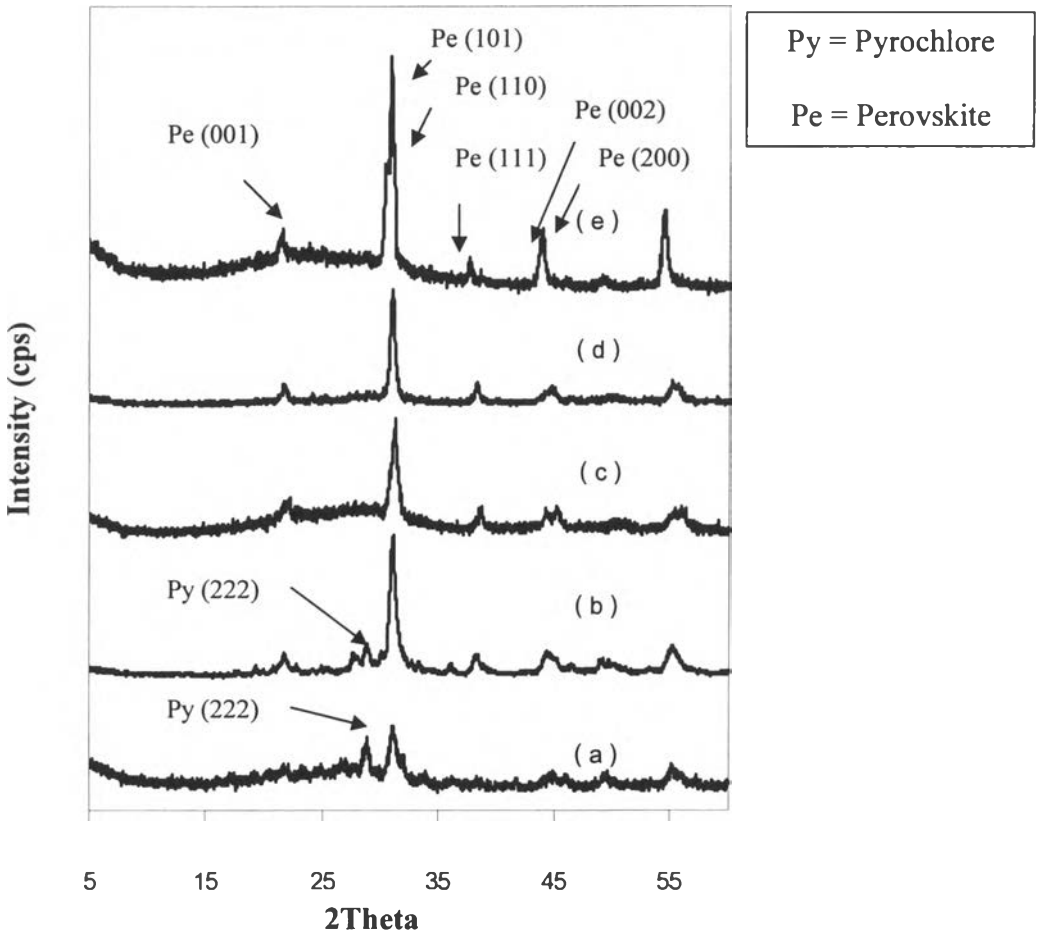

Figure 4.13 XRD pattern of calcined PZT for 1.5 h at (a) 600°, (b) 700°, (c) 800°, (d) 900° and (e) 1100°C.

Wu *et al.* (1997) reported that the pychochlore and perovskite phases were sequentially formed in the sol-gel derived PZT during crystallization, even at a low thermal treatment about 500°-600°C, a mixture of both pyrochlore and perovskite phases was still formed. At higher temperature about 700°-750°C, the pure perovskite phase was obtained.

Composition analysis of calcined PZT was performed on a EDS/SEM spectrometer and the results are listed in Table 4.7.The exact composition of Pb was not exactly obtained due to the Pb loss during irridiation by the electron beam (Reaney *et al.*, 1994). However, the Zr/Ti ratio was close to the calculated value and

composition percentages decreased with increasing temperature. As expected, the Pb value significantly decreased with temperature.

Table 4.7 Composition of calcined PZT by the sol-gel process

Calcined Temp. (°C)	Elemental Composition (atomic %)				Zr/Ti
	O	Pb	Ti	Zr	
Calculated					1.875
700	89.96	5.72	1.58	2.74	1.734
800	93.23	2.58	1.47	2.72	1.850
900	96.17	1.37	0.86	1.60	1.861
1100	96.78	1.08	0.75	1.38	1.840

4.8 Characterization of Uncalcined PZT via the Sol-Gel Process and Microwave Technique

FTIR spectrum of calcined PZT powder after heated with microwave shows C-H bonds at 3000-2800 and 1456 cm^{-1}, meaning that although microwave heating was used, organic part was still there. However, the FTIR spectrum also shows peaks of M-O-M and M-O at 993-866 and 560 cm^{-1} (Caruso *et al.*, 1999 and Barton and Ollis, 1979), respectively, indicating that some of PZT product formed via the microwave technique.

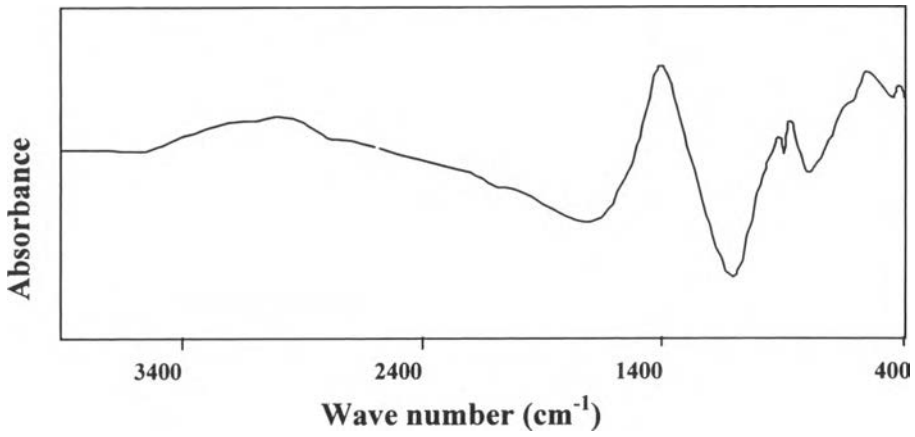

Figure 4.14 FTIR spectrum of uncalcined PZT via the sol-gel process and microwave technique.

The thermal properties of uncalcined PZT powder via the sol-gel process and the microwave technique analyzed by TGA and DTG under air atmosphere at the heating rate of 10°C/min are shown in Figure 4.15. An exothermic peak in the temperature range of 100°C is due to water residue and the peak at 200°-400°C corresponds to some organic groups (Caruso *et al.*, 1999). At higher temperatures, two exothermic peaks, which were also accompanied by mass loss and changes in the DTG, at 400°-500°C and 580°-650°C indicated the pyrochloric and perovskite phase formation, respectively (Lee *et al.*, 2002 and Livage *et al.*, 1994). The temperature needed to form perovskite was lower than uncalcined PZT obtained from using only the microwave technique.

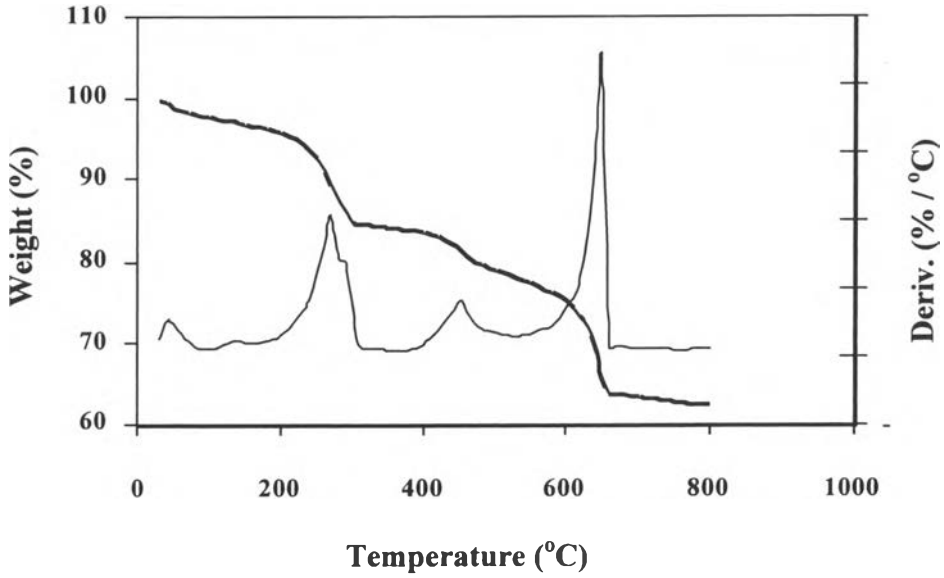

Figure 4.15 TGA/DTG of uncalcined PZT via the sol-gel process and microwave Technique.

Lee *et al.* (2002) and Towata *et al.* (2002) studied the seeding effect on the phase transformation of PZT. By introducing PZT seeding in the PZT sol-gel system, polycrystalline PZT powders in pure perovskite phase could be obtained at 550°C, which was about 100°C lower than the unseeded case. Similarly, PZT obtained via the sol-gel and microwave techniques also required lower temperature to form pure perovskite phase at the temperature close to the seeding PZT sol-gel system.

SEM shows different morphologies between the uncalcined PZT after heated with microwave and the uncalcined PZT after gone through the sol-gel process without microwave technique. The obtained particles were larger and the density surface increased, as shown in Figure 4.16.

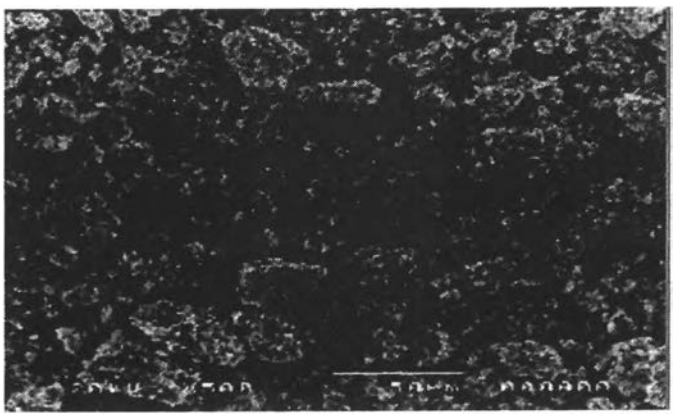

Figure 4.16 SEM micrograph of unclacined PZT powder after heated with microwave.

4.9 Characterization of Calcined PZT via the Sol-Gel Process and Microwave Technique

FTIR spectrum (Figure 4.17) clearly shows only M-O-M and M-O peaks at 1005, 560 -418 cm^{-1}, respectively, when calcined PZT at 900°C for 1.5 h. The FTIR spectra of Caruso *et al.* (1999) showed the evolution of the hydroxyl and organic residues in the temperature range of 200°-400°C. At 400°C peaks of M-O-M and M-O were low in intensity.

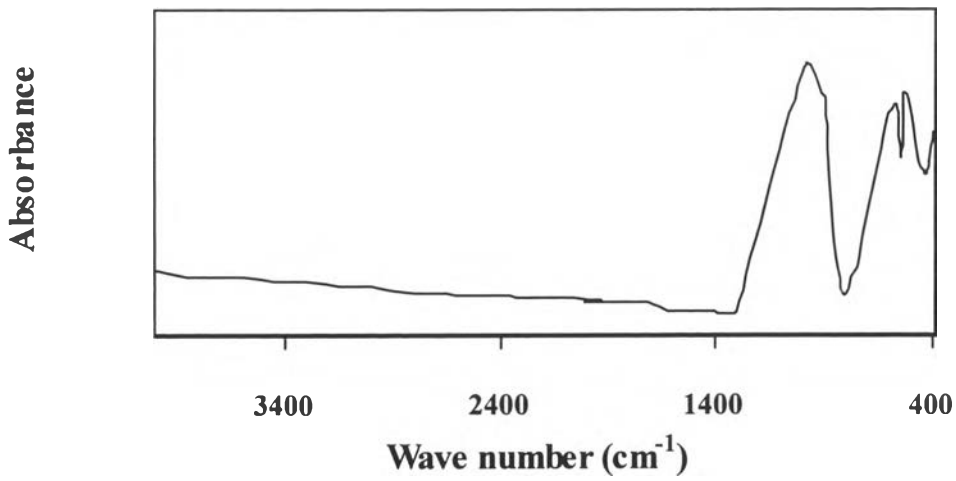

Figure 4.17 FTIR spectrum of calcined PZT via the sol-gel process and microwave technique.

Figures 4.18 shows macro particles of PZT after calcined at 900°C, the macro particles were larger than uncalcined one. That means, higher temperature had effect on the macromolecular size and crystallinity of the PZT product.

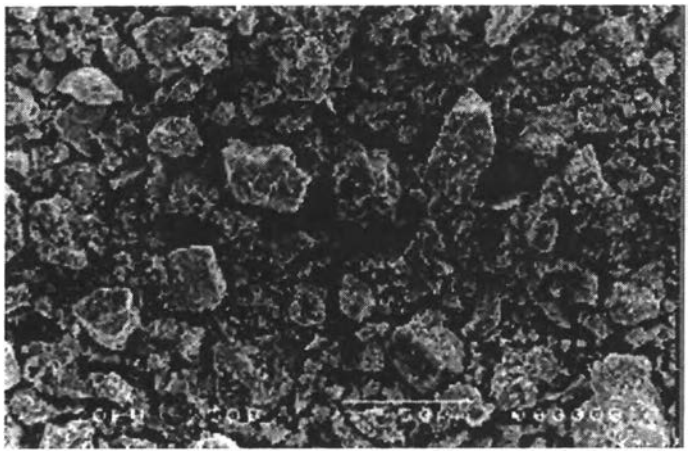

Figure 4.18 SEM morphology of calcined PZT at 900°C by the sol-gel process and microwave technique.

Chang *et al.* (2002) reported that the cracked surface, the density surface and the grain size decreased at 850°C for 5 min. They concluded that very high calcined temperature was not suitable, the optimum time was 20 min at 650°C of calcined temperature. In our case, from Table 4.8 low surface areas of PZTobtained via the sol-gel process, the microwave technique and the calcination at 900°C were impressive and appear to be crystalline, they had high density surface and were thermally stable. The time in microwave had affected the grain size and the surface area. If PZT was heated for a long time in microwave, the surface area decreased but the density surface and the grain size increased.

Table 4.8 Surface area of calcined PZT at 900°C for 1.5 h via the sol-gel process for various times in microwave

Time in Microwave (h)	Surface Area (m^2/g)
5	22.00
10	18.97
15	15.10
20	12.20
25	9.09

The gels obtained from heating the sols with a microwave at 150°C for 5, 10, 15, 20 and 25 h were calcined at 900°C for 1.5 h. The calcined products were investigated for their structures using XRD. As shown in figures 4.19, the longer microwave heating time yielded the higher intensity and the purer perovskite products. The intensity of XRD was used to determine the phase formation, and the lattice constants of the materials were determined by the diffraction value (Table 4.9).

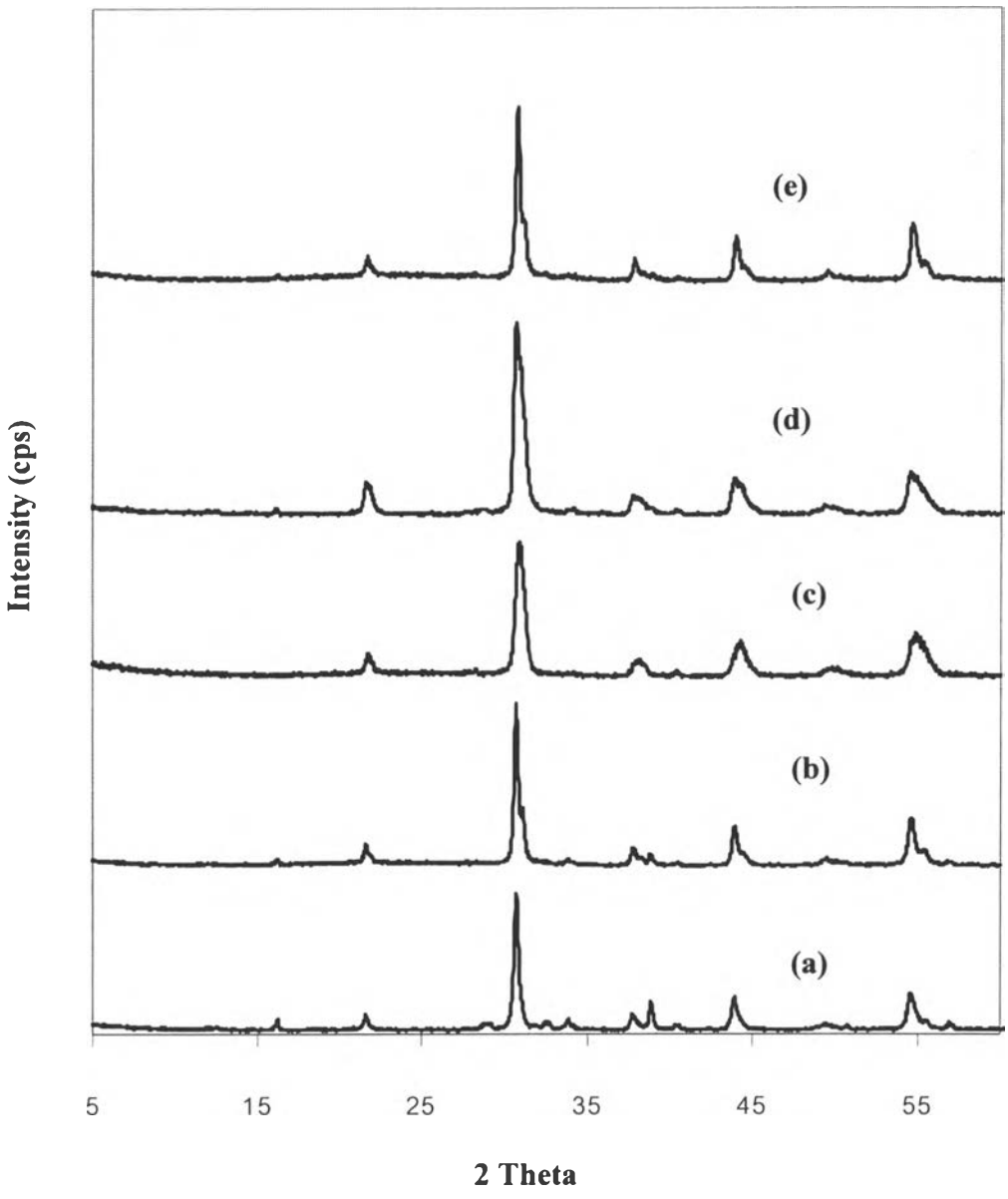

Figure 4.19 XRD patterns of PZT heated by microwave for (a) 5, (b) 10, (c) 15, (d) 20 and (e) 25 h followed by calcination at 900°C for 1.5 h.

Table 4.9 Relative inensity and % perovskite content of PZT heated by microwave followed by calcination at 900°C for 1.5 h

Time in microwave (h)	Intensity (cps)		Perovskite Content (%)
	Pe (110)	Py (222)	
5	522	205	71.80
10	981	-	100.00
15	1164	-	100.00
20	1352	-	100.00
25	1489	-	100.00

Intensity of XRD and the % Perovskite content increased with increasing microwave heating time. XRD pattern from Figure 4.19 was used to determine the lattice constants of PZT (0.52:0.48) obtained via the sol-gel process and the microwave techniques at 150°C for 25 h followed by calcination at 900°C for 1.5 h. The 001 and 100 reflections were chosen to determine the lattice constant, as shown in Table 4.10, indicating the tetragonal structure. The spacing parameter d and the lattice constant of tetragonal and rhombohedral of PZT structure were calculated using equations (4.1) and (4.2), respectively.

$$\frac{1}{d^2_{hkl}} = \frac{h^2 + k^2}{a^2} + \frac{l^2}{c^2} \qquad (4.1)$$

$$\frac{1}{d^2_{hkl}} = \frac{(h^2 + k^2 + l^2)\sin^2\alpha + 2(hk + kl + lh)(\cos^2\alpha - \cos\alpha)}{a^2(1+2\cos^3\alpha - 3\cos^2\alpha)} \qquad (4.2)$$

Glazer et al [33] reported that the rhombohedral angle (α) of simple perovskite struture was 89.772°, and thus the value was used in our work.

Table 4.10 $d_{h\,k\,l}$ of PZT (0.52:0.48) via the sol-gel process and microwave technique at 150°C for 25 h, calcined at 900°C for 1.5 h. comparison between tetragonal and rhombohedral structure

Input a = 4.1070 and c = 4.1259 in Eq (4.1)

a. = 4.1259 and α = 89.772 in Eq (4.2)

h	k	l	d (observed)	d (calculated)	
				Tetragonal	Rhombohedral
0	0	1	4.1259	4.1259	4.1259
0	1	0		4.1070	4.1259
1	0	0	4.1070	4.1070	4.1259
1	0	1	2.9062	2.9107	2.9232
0	1	1		2.9107	2.9232
1	1	0	2.8697	2.9041	2.9232
1	1	1	2.3732	2.3748	2.3916
0	0	2	2.0562	2.0629	2.0629
0	2	0		2.0535	2.0629
2	0	0	2.0317	2.0535	2.0629
1	0	2	1.8411	1.8434	1.8479
0	1	2		1.8434	1.8479
2	0	1	1.8399	1.8384	1.8479
1	1	2	1.6789	1.6818	1.6865

If the heating time in microwave was constant and the calcination temperature was varied, the best condition to synthesize PZT would be found. In Figure 4.20, heating time in microwave was10 h at 150°C and the calcination temperature was varied at 700°, 800°, 900°, 1100° and 1300°C for 1.5 h, as listed in Table 4.11, the % Perovskite content was 100 % and the intensity was high. In generally at high temperature PbO is volatilized [28, 29], resulting in the PZT phase

change, and thus intensity and % Perovskite content should decrease. However, it is not true in our case. The reason is probably due to the stability of the PZT product at higher temperature.

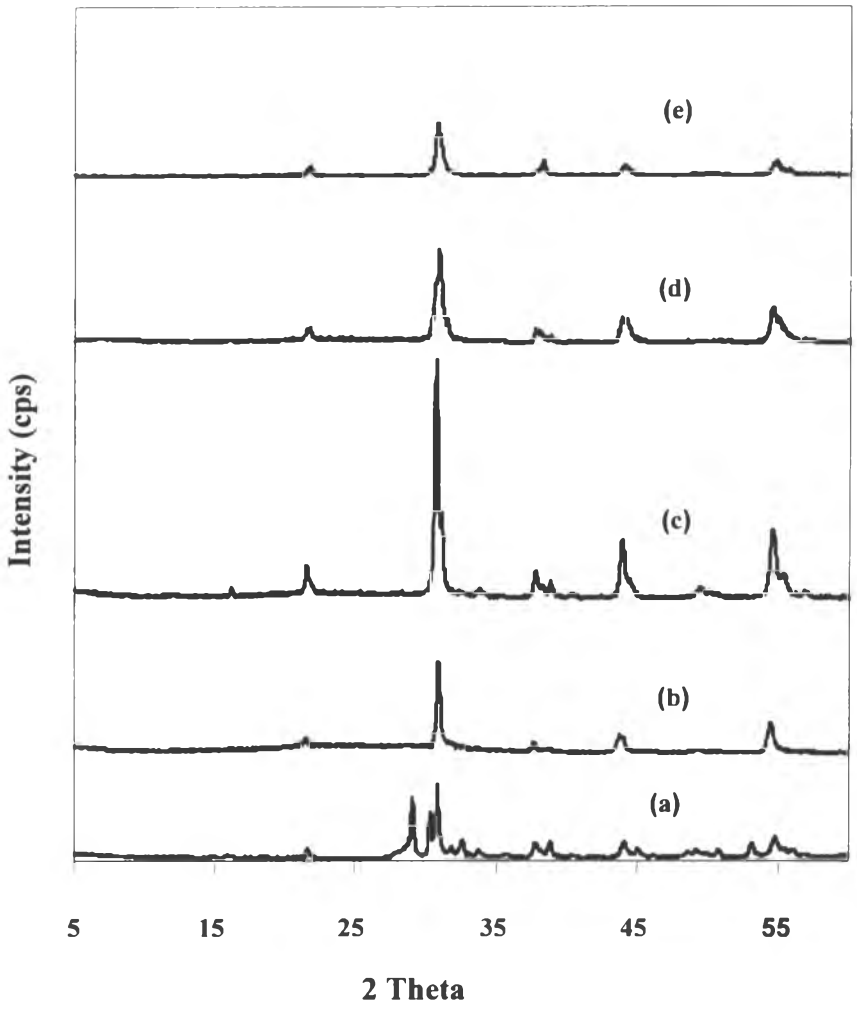

Figure 4.20 XRD patterns of PZT via the sol-gel process and microwave technique for 10 h and calcined (a) 700°, (b) 800°, (c) 900°, (d) 1100° and (e) 1300°C.

Table 4.11 Relative inensity and % perovskite content of PZT heated by microwave at 150°C for 10 h followed by calcinations at various temperatures

Calcined Temp. (°C)	Intensity (cps)		% Perovskite Content
	Pe (110)	Py (222)	
700	2231	1234	64.38
800	1031	-	100.00
900	1489	-	100.00
1100	892	-	100.00
1300	503	-	100.00

Composition analysis to prove the percentages of elements in PZT using SEM/EDS provided values close to the calculated ones. For the effects of microwave heating time (Table 4.12) and calcinations temperature (Table 4.13), the Zr/Ti ratios of PZT were also close to the calculated ones, except the product with calcination temperature higher than 1300°C. The Zr/Ti ratio ratio decreased because of the volatization of Pb, Ti and Zr [11,30].

Table 4.12 Composition of PZT via the sol-gel process and microwave technique at 150°C followed by calcination at 900°C for 1.5 h

Time in microwave (h)	Elemental Composition (atomic %)				Zr/Ti
	O	Pb	Ti	Zr	
Calculated					1.875
5	88.17	5.10	2.37	4.36	1.840
10	89.41	4.36	2.18	4.05	1.858
15	90.18	4.11	2.00	3.71	1.855
20	91.23	3.67	1.78	3.32	1.865
25	91.24	3.34	1.54	2.88	1.870

Table 4.13 Composition of PZT via the sol-gel process and microwave technique at 150°C for 10 h, at various calcination temperatures

Calcined Temp. (°C)	Elemental Composition (atomic %)				Zr/Ti
	O	Pb	Ti	Zr	
Caculated					1.875
800	87.38	5.30	2.60	4.72	1.815
900	89.41	4.36	2.18	4.05	1.858
1100	95.93	1.73	0.82	1.52	1.854
1300	97.56	0.79	0.59	1.06	1.797

4.10 Characte rization of Calcined PZT(0.52:0.48) via the Sol-Gel Process, using Pb Acetate in place of Pb Glycolate precursor

The power X-ray diffraction was used to determine a lattice constant of PZT (0.52:0.48) synthesized using Pb acetate precursor to compare with Pb glycolate precursor. A mixture of Ti glycolate, Zr glycolate and Pb acetate was prepared using the same condition as that of Pb, Ti and Zr glycolates. PZT gel was calcined at 800° and 900°C for 1.5 h. XRD patterns shown in Figure 4.21 and Table 4.14 indicate the rhombohedral structure whereas PZT synthesized using Pb glycolate, in Figure 4.19 and Table 4.10, gives the tetragonal structure. The spacing parameter d and the lattice constant of tetragonal and rhombohedral of PZT structure were calculated using equations (4.1) and (4.2), respectively (Schwartz *et al.*, 1997).

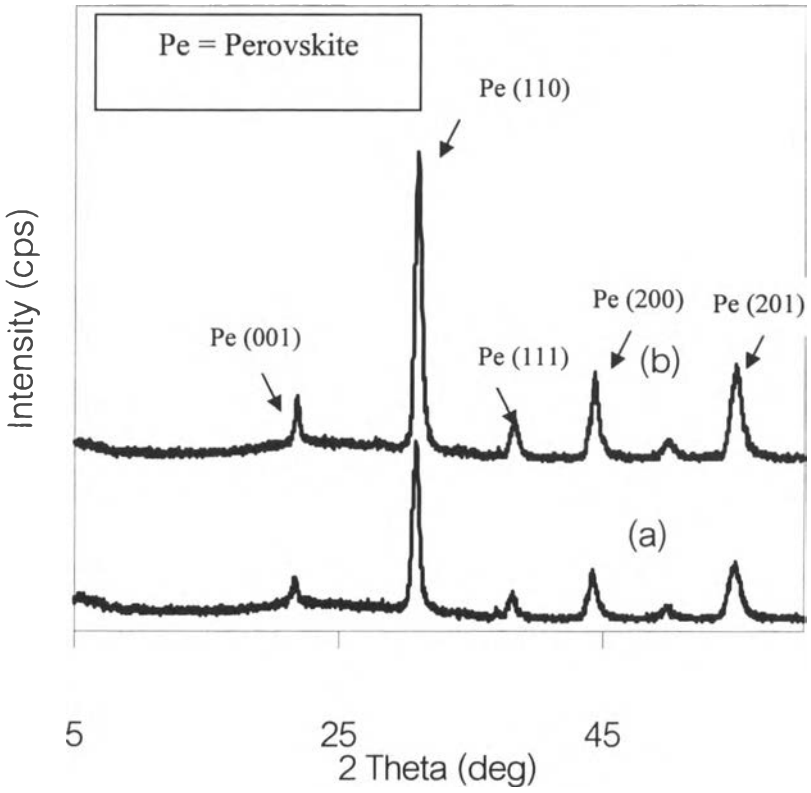

Figure 4.21 XRD patterns of PZT (0.52:0.48) obtained via the sol-gel process, using Pb acetate precursor and calcined at (a) 800° and (b) 900°C for 1.5 h.

Table 4.14 $d_{h\,k\,l}$ of PZT (0.52:0.48) obtained via the sol-gel process, using Pb acetate precursor and calcined at 900°C for 1.5 h

Input a. = 4.0772 and α = 89.772 in eq (4.2)

h	k	l	d (observed)	d (calculated) Rhombohedral
0	0	1	4.0772	4.0771
0	1	0		4.0771
1	0	0		4.0771
1	1	0	2.8878	2.8886
0	1	1		2.8886
1	0	1		2.8886
1	1	1	2.3552	2.3633
0	0	2		2.0448
2	0	0	2.0385	2.0448
0	2	0		2.0448
1	0	2		18.254
2	0	1	1.8262	18.254
2	1	0		18.254
1	1	2	1.6699	1.6700